Environmental Science & Technology

Article

Cite This: Environ. Sci. Technol. 2019, 53, 2396−2404

pubs.acs.org/est

Functionalized Anion-Exchange Membranes Facilitate Electrodialysis of Citrate and Phosphate from Model Dairy Wastewater

Laura Paltrinieri,*[,†,‡] Elisa Huerta,[§] Theo Puts,[§] Willem van Baak,[§,#] Albert B. Verver,[∥] Ernst J.R. Sudhölter,[†] and Louis C. P. M. de Smet*[,†,‡,⊥]

[†]Delft University of Technology, Department of Chemical Engineering, Van der Maasweg 9, 2629 HZ Delft, The Netherlands

[‡]Wetsus−European centre of excellence for sustainable water technology, Oostergoweg 9, 8932 PG Leeuwarden, The Netherlands

[§]FUJIFILM Manufacturing Europe BV, Oudenstaart 1, 5000 LJ Tilburg, The Netherlands

[∥]FrieslandCampina, Stationsplein 4, 3818 LE Amersfoort, The Netherlands

[⊥]Wageningen University & Research, Laboratory of Organic Chemistry, Stippeneng 4, 6708 WE Wageningen, The Netherlands

Supporting Information

ABSTRACT: In this study, the preparation of a new, functional anion-exchange membrane (AEM), containing guanidinium groups as the anion-exchanging sites (Gu-100), is described as well as the membrane characterization by XPS, water uptake, permselectivities, and electrical resistances. The functional membrane was also employed in pH-dependent electrodialysis experiments using model dairy wastewater streams. The properties of the new membrane are compared to those of a commercially available anion-exchange membrane bearing conventional quaternary ammonium groups (Gu-0). Guanidinium was chosen for its specific binding properties toward oxyanions: e.g., phosphate. This functional moiety was covalently coupled to an acrylate monomer via a facile two-step synthesis to yield bulk-modified membranes upon polymerization. Significant differences were observed in the electrodialysis experiments for Gu-0 and Gu-100 at pH 7, showing an enhanced phosphate and citrate transport for Gu-100 in comparison to Gu-0. At pH 10 the difference is much more pronounced: for Gu-0 membranes almost no phosphate and citrate transport could be detected, while the Gu-100 membranes transported both ions significantly. We conclude that having guanidinium groups as anion-exchange sites improves the selectivity of AEMs. As the presented monomer synthesis strategy is modular, we consider the implementation of functional groups into a polymer-based membrane via the synthesis of tailor-made monomers as an important step toward selective ion transport, which is relevant for various fields, including water treatment processes and fuel cells.

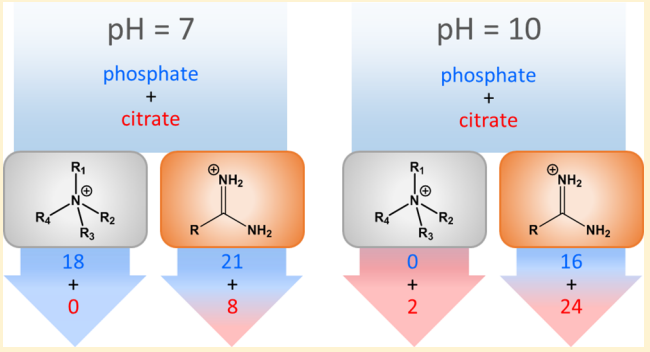

INTRODUCTION

Providing innovative separation technologies for a sustainable water supply is a key challenge facing society.[1,2] Electrical-driven-based technologies such as electrodialysis (ED),[3] membrane capacitive deionization (MCDI),[4,5] and reverse electrodialysis (RED)[6] are efficient and versatile systems for water treatment that can effectively overcome the global need for the supply and reuse of water. The aforementioned technologies rely on the use of ion-exchange membranes (IEMs) as the core of the separation process. Under applied current or potential, cations can cross cation-exchange membranes (CEMs) while anions can permeate through anion-exchange membranes (AEMs), resulting in an alternating concentrated and depleted compartment. IEMs have been employed extensively in several sectors such as brine concentration,[7] wastewater treatment,[8] nutrient recovery,[9] organic compound separation,[10] mineral production from acids and bases,[11] and acid production.[12] Most recently, IEMs have been used for the ED of dairy industrial effluents as an advanced food processing technology.[13] The process has been applied for the separation of various ions, including lactate,[14] citrate,[15] potassium,[16] magnesium,[16] sodium,[17] chloride,[17] and phosphate.[18] Thus, ED effectively removes ions from various feed streams, but typically IEMs exhibit a low selectivity when they are exposed to complex matrix solutions. High selectivities toward specific ions are required when the final goal is the recovery and reuse of the target compounds. Although

Received: October 2, 2018
Revised: November 23, 2018
Accepted: November 28, 2018
Published: December 21, 2018

DOI: 10.1021/acs.est.8b05558
Environ. Sci. Technol. 2019, 53, 2396−2404

Scheme 1. Reaction Scheme for the Two-Step Synthesis of (1) Guanidinium Propanol and (2) the Guanidinium Acrylate Monomer

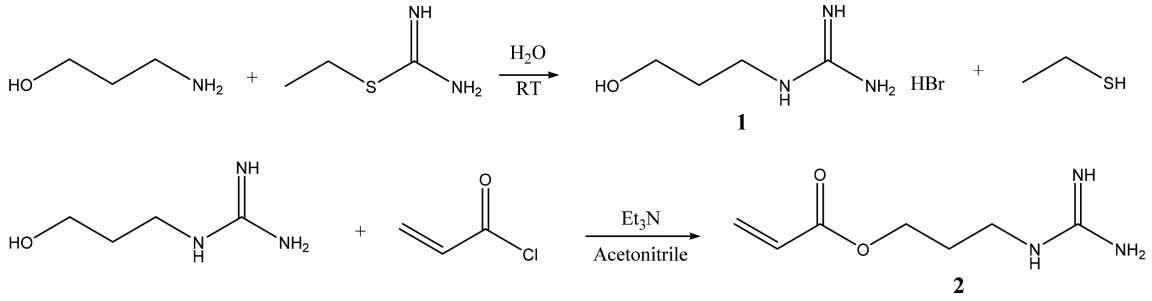

variations of operational parameters (e.g., current density, flow rate, stack design) can provide a certain control over ion transport, tuning the (perm)selectivity properties of IEMs by synthetic approaches is becoming of increasing interest and importance.[19] Over the past few years, several research groups started investigating the fabrication and/or modification of IEMs to increase their selectivity. Often used are polyelectrolytes, which are deposited as multilayers on top of IEMs to improve monovalent/divalent selectivity: for example K^+/Mg^{2+}, Cl^-/SO_4^{2-}, or Cl^-/Ca^{2+}.[20−22] Other methods involve the use of monomers grafted at membrane surfaces to reduce co-ion permeability[23] or to facilitate permeation of certain compounds, such as urea.[24] Recently nanoparticles have been incorporated in the IEM to improve Na^+/Ba^{2+} transport.[25] While these studies nicely show the potential of functionalizing membranes to tune selectivity, most of the experiments are carried out with solutions containing only two different salts, reflecting a strong simplification of industrially relevant conditions.

In this study, we developed a new AEM exclusively composed of receptor groups and we examined the ion-selective properties, in comparison with a commercial AEM, on exposure to a complex model dairy solution. In more detail, to improve the membrane ion-transport performances, we synthesized an acrylate monomer containing a guanidinium receptor (Gu) as a building block for the AEM fabrication via UV polymerization. Gu can form preferential bonds with oxyanions,[26−28] which are abundant in dairy effluents. In addition, Gu is a versatile group which can be easily functionalized with specific chemical groups, in this case an acrylate. Gu has been already combined with AEM to enhance alkaline stability[29−31] or to increase membrane conductivity.[32] However, research on the integration of functional groups, such as Gu, with membranes aiming to improve ion selectivity is in its infancy. Recently, we blended a Gu-based polyelectrolyte with AEM building blocks to prepare a functionalized AEM, aiming to facilitate $H_2PO_4^-/SO_4^{2-}$ transport.[33] The addition of 8 wt % of functionalized polyelectrolyte resulted in an increased permeation of phosphate over sulfate on application in electrodialysis. In the current study, the electrochemical properties of a Gu-functionalized AEM of which the fixed charges are exclusively due to the presence of the covalently linked Gu groups were investigated in detail and correlated with the observed membrane selectivity performances. The membranes were investigated using a model dairy wastewater composition.

MATERIALS AND METHODS

Materials. All chemicals listed in this section were used as received, unless stated otherwise. 3-Amino-1-propanol, 2-ethyl-2-thiopseudourea, acryloyl chloride, and triethylamine were purchased from Sigma-Aldrich and used for the synthesis of the guanidinium acrylate monomer. Acetonitrile (anhydrous, 99.8%, Sigma), ethyl acetate (anhydrous, 99.8%, Sigma), ethanol (BioUltra >99.8%, Sigma), methanol (anhydrous, 99.8%, Sigma), and Milli-Q water (Millipore, 18.2 MΩ cm^2, T = 24.5 °C) were used as solvents during the synthetic steps. A standard grade AEM, having quaternary ammonium as fixed charged groups, from Fujifilm Manufacturing Europe BV (The Netherlands, hereafter Fuji) was selected as a reference membrane. To obtain a guanidinium acrylate based membrane, we used *N*,*N*-methylenebis(acrylamide) (99% Sigma) as cross-linker, 2-hydroxy-2-methyl-1-phenyl-1-propane (Darocure1173, Ciba Specialty Chemicals) as the free radical photoinitiator, TEGO Glide (Evonik) as the surfactant, and hydroquinone monomethyl ether (MEHQ) as an inhibitor, and a polypropylene nonwoven material was used as the substrate for the membrane formation during the UV polymerization. Demi water and isopropyl alcohol (Sigma) were used as solvents during membrane fabrication. Sodium phosphate monobasic monohydrate (>98%, $NaH_2PO_4{\cdot}H_2O$, Across Organic), sodium phosphate dibasic (Na_2HPO_4, 99.95%, Sigma), sodium sulfate (>99%, Na_2SO_4, Sigma), sodium chloride (NaCl, 99.5%, Sigma), sodium citrate tribasic hydrate (ReagentPlus, >99%, Sigma), and sodium L-lactate (98%, Sigma) were used to prepare the model aqueous dairy solutions.

Monomer Synthesis. Scheme 1 shows the two-step synthesis developed to obtain the guanidinium acrylate monomer. Guanidinopropanol (**1**) was synthesized according to Funhoff et al.[34] In detail, 8.54 mmol of 3-aminopropanol was slowly added to 8.54 mmol of 2-ethyl-2-thiopseudourea hydrobromide in a 100 mL flask. Subsequently, 2 mL of Milli-Q water was added. The solution was stirred overnight at room temperature. Next, water was removed under reduced pressure to obtain a viscous transparent liquid (yield 16.47 mmol, 96%). For the synthesis of the guanidinium acrylate monomer (**2**), compound **1** (1.67 g = 8.43 mmol) was stirred in acetonitrile (5 mL) at room temperature for 1 h. Freshly activated molecular sieves (4 Å, Sigma) were added to the solution in order to remove residual amounts of water. Triethylamine (0.85 mL = 8.43 mmol) was added dropwise, followed by the dropwise addition of 0.76 mL (8.43 mmol) of acryloyl chloride. The solution was stirred for 24 h and kept in an ice bath to avoid prepolymerization. The acetonitrile was removed under vacuum. Product **2** was washed with EtAc/EtOH (1/1)

DOI: 10.1021/acs.est.8b05558
Environ. Sci. Technol. 2019, 53, 2396−2404

to remove any Et_3N and filtered to remove the molecular sieves. Purification was done by column chromatography using MeOH/EtAc (20/80) as eluent. ^{1}H NMR spectra were recorded using a Bruker AVANCE 400 NMR spectrometer with D_2O as solvent. For **2** the following ^{1}H NMR (CD_3OD) was obtained (δ (ppm)): 7.4 (s, 1H, NH), 6.8 (s, 1H, NH), 6.4 (d, 1H, CH, J = 17.2 Hz), 5.8 (d, 1H, CH, J = 10.5 Hz), 6.1 (m, 1H, CH, J = 27.7 Hz), 4.2 (t, 2H, CH_2, J = 12 Hz), 3.2 (t, 2H, CH_2, J = 13.9 Hz), 1.9 (m, 2H, CH_2, J = 23.7 Hz). Yield: 1.64 mmol, 40 wt %. The molecular mass of **2** was confirmed by liquid chromatography-mass spectrometry (LCMS; Shimadzu 2010A LCMS, ESI/APCI), as it yielded m/z $[M + H]^+$ 171.80. The FT-IR spectrum of **2** was obtained using a Nicolet 8700 FT-IR instrument. The spectrum was recorded over a range of 4000−400 cm^{-1} at a resolution of 4 cm^{-1}.

Membrane Fabrication. The guanidinium acrylate based AEM was prepared via a UV-polymerization reaction initiated by free radicals from the active double bonds of the Darocure1173 photoinitiator. In detail, 0.053 mol of **2** and 0.017 mol of cross-linker were added to 2 mL of demi water and 1.7 mL of isopropyl alcohol and mixed until a clear solution was obtained. Next, 1 wt % of TEGOGlide, 1 wt % of MEHQ, and 0.05 wt % of Darocure1173 were added to the mixture. The mixture was cast into films by coating a nonwoven polypropylene substrate with a 12 μm wire-wound coating bar. The membrane was exposed to UV irradiation (240 W/cm) through a benchtop conveyor system (Heraeus Noblelight Fusion UV inc. USA). A mercury H bulb (240−280 nm) working at 100% intensity was used, and the conveyor speed was 30 m min^{-1} with a single pass. The obtained membrane was referred to as Gu-100, indicating that 100% of the exchange sites are Gu groups. The membrane formulation was prepared such that the amount of exchange sites was comparable to the amount of quaternary groups present in the reference AEM, i.e., a standard grade Fuji membrane, here referred to as Gu-0 (2.71 and 2.83 mmol g^{-1} for Gu-100 and Gu-0, respectively). The membrane thickness was found to be 142 ± 2 μm for Gu-0 and 148 ± 2 μm for Gu-100 as measured with a digital screw micrometer (Mitutoyo Corporation, Japan, Model 293-240-30).

Membrane Characterization. The membrane water uptake (w_{uptake}) was determined by application of the equation[35]

$$w_{uptake} = \frac{m_{wet} - m_{dry}}{m_{wet}} (\%) \quad (1)$$

where m_{wet} and m_{dry} are the membrane masses in the wet and dry state, respectively. The wet mass was obtained after immersing the membrane in Milli-Q water for 48 h. The excess of water on the membrane surface was quickly removed using laboratory wipes. For the dry mass, samples were dried in a vacuum oven at 50 °C for 48 h. The w_{uptake} value is reported as an average of the measurements for three different membranes.

Elemental composition by X-ray photoelectron spectroscopy (XPS, Thermo Fisher Scientific, K-Alpha model) was used to determine the surface atomic composition of Gu-100 and Gu-0 membranes. A monochromatic Al Kα X-ray source with a spot size of 400 μm at a pressure of 10^{-7} mbar and a constant pass energy of 400 eV for the survey spectra and 50 eV for the detailed high-resolution spectra were used. The flood gun was turned on during the measurement to compensate for potential charging of the surface. The peak position was adjusted on the basis of the internal standard C 1s peak at 284.8 eV, with an accuracy of ±0.05 eV. Avantage processing software was used to analyze all spectra.

Membrane permselectivity (PS) values indicate to what extent counterions (anions) are transported through the membrane and co-ions (cations) are rejected and was determined from the deviation of the experimentally observed membrane potential in comparison to the calculated membrane potential for 100% permselective membranes (Nernst potential), using the Donnan theory.[36] We measured the PS for a selected number of anions as shown in Table 1:

Table 1. Composition of Model Dairy Wastewater Used in the Experiments and Their Conjugated pK_a Values, Diffusion Coefficients (D), and Stokes Radii (r_s)[45]

anion[a]	amt (mmol)	pK_a	D (10^{-5} cm^2 s^{-1}[b])	r_s (Å)
chloride	30	−7	2.032 [−1]	1.21 [−1]
phosphate	10	2.13; 7.21; 12.32	0.959 [−1]; 0.759 [−2]	2.6 [−1]; 2.4 [−2]
citrate	10	3.13; 4.76; 6.40	0.623 [−3]	3.8 [−3]
lactate	1	3.78; 15.1	1.033 [−1]	2.3 [−1]
sulfate	1	−3; 1.99	1.065 [−2]	2.3 [−2]

[a]All as sodium salts. [b]Values in brackets indicate the ionic charge.

chloride, a monovalent anion commonly used as a reference and abundantly present in dairy effluent; phosphate, a pH-dependent anion (here measured both at pH 5 and pH 10); sulfate, a representative divalent anion. Anions were measured separately for a total of four individual experiments, and the concentrations were 0.05 and 0.5 M for each compartment, respectively. Since no current is applied during the PS experiment, ion transport through the membrane is mainly determined by diffusion.[35,37] Membrane PS was determined with a two-compartment cell[38] (custom-made by STT Products, The Netherlands), as illustrated in Figure S1 of the Supporting Information. The membrane was placed in the sample holder with an effective cross-sectional area of 8.14 cm^2 separating two salt solutions. The potential difference between two Ag/AgCl double-junction reference electrodes (Methrom, The Netherlands) separated with the membrane under investigation (E_x) was measured with a digital multimeter (Digimess). The potential was read out after stabilization was reached (typically after 3−5 min). The experimental membrane potential (E_m) was then obtained by subtracting the offset potential (E_{offset}) of the electrodes, measured in 3 M KCl solutions:[38,39]

$$E_m = E_x - E_{offset} \text{ (mV)} \quad (2)$$

The final value of permselectivity (%PS) was calculated as the ratio between the experimentally determined E_m and the theoretically calculated Nernst potential (E_{Nernst}) for 100% permselectivity:[38,39]

$$PS = \frac{E_m}{E_{Nernst}} \times 100 (\%) \quad (3)$$

E_{Nernst} was calculated using the formula

$$E_{Nernst} = \frac{RT}{nF} \ln \frac{C_1\gamma_1}{C_2\gamma_2} \text{ (mV)} \quad (4)$$

where R is the gas constant, T is the temperature in Kelvin, F is the Faraday constant, n is the valency of the transferring ion,

DOI: 10.1021/acs.est.8b05558
Environ. Sci. Technol. 2019, 53, 2396−2404

and $C_1\gamma_1$ and $C_2\gamma_2$ are the concentrations and activity coefficients of the transferring anion in the diluted and the concentrated compartment, respectively. The electrolyte solutions were continuously recirculated by using two peristaltic pumps (Masterflex Peristaltic pumps, model L/S Economy Pump System with Easy-Load II pump head 230 VAC, The Netherlands) keeping a constant flow rate of 110 mL/min in each compartment. A thermal bath (Thermo Fisher Scientific Inc., USA) was used to maintain a constant temperature of 20 ± 0.5 °C.

Membrane electrical resistance (ER) was measured for Gu-100 and Gu-0, and the values reflect the ion mobilities in the membrane. The higher the resistance, the lower the ion mobility.[40,41] Obviously, a low membrane resistance is preferred. The ER was determined by using a conventional six-compartment cell (custom-made by STT Products, The Netherlands).[40] Membranes between compartments were placed according to the configuration shown in Figure 1. ER

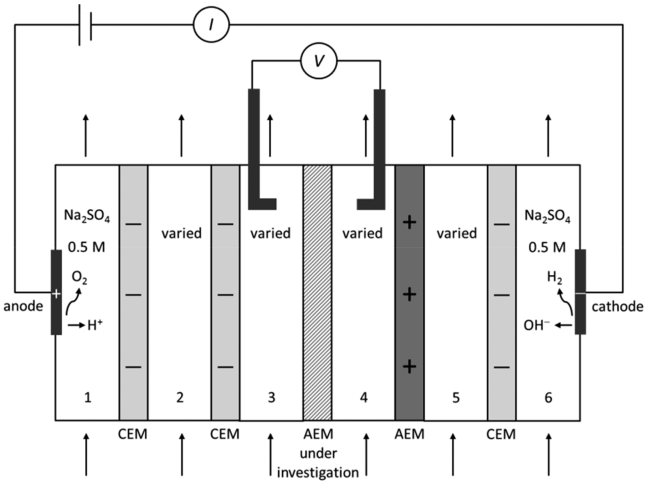

Figure 1. Scheme of the setup used to perform electrochemical impedance spectroscopy and electrodialysis experiments. CEM and AEM denote cation- and anion-exchange, standard-grade membranes, respectively. The membrane under investigation was positioned between compartments 3 and 4. The current was supplied from two counter electrodes positioned in compartment 1 (anode) and compartment 6 (cathode).

was determined with a four-electrode configuration with chronopotentiometry measurements by applying a direct current increased step by step (i.e. 0, 0.05, 0.06, ..., 0.3 s and every 30 s) via a power supply (Autolab, potentiostat/galvanostat PGSTAT302N).[42] The voltage across the membrane under investigation was measured with a voltage meter through Haber−Luggin capillaries. Compartments containing the anode and cathode (compartments 1 and 6 in Figure 1) were filled with 0.5 M Na_2SO_4 solution, and the other compartments contained NaH_2PO_4 (at pH 5), Na_2HPO_4 (at pH 10), NaCl, and Na_2SO_4, which were measured separately at a concentration of 0.5 M for a total of four experiments. Electrolyte solutions were circulated individually at the same flow rate of 250 mL min^{-1}, and the temperature was fixed at 25 ± 0.5 °C by using a thermal bath (Thermo Fisher Scientific Inc., USA). Prior to the analysis a blank measurement without a membrane was made, and the registered value was subtracted from each measurement. Before use, the membranes were equilibrated for 48 h in the same salt solution used in the analysis.

Electrodialysis of Model Dairy Wastewater. Electrodialysis (ED) was performed on both Gu-0 and Gu-100, using the setup as shown in Figure 1. Table 1 gives the composition of the model dairy solution. Table 2 reports the calculated

Table 2. Calculated Percentages of Phosphate and Citrate Speciation at Different pH Values

anion	pH	monovalent (%)	divalent (%)	trivalent (%)
phosphate	5	100	0	0
	7	62	38	0
	10	0	100	0
citrate	5	35	61	4
	7	0	19	81
	10	0	0	100

percentage of phosphate and citrate speciation at the selected pH values. The dairy model solution was used to fill compartments 2−5, while a solution of 0.5 M Na_2SO_4 was circulated through the compartments of the cathode and anode electrodes (i.e., compartments 1 and 6). All solutions were continuously pumped at 110 mL min^{-1} at a fixed temperature of 25 °C by using the peristaltic pump and the thermostatic bath as described in the previous section. The pH was monitored in the feed and the receiving compartments during permeation experiments and was set around pH 7, chosen as a representative pH value of dairy effluent. In addition, also measurements at pH 10 were performed, where divalent phosphate is the dominant species, in order to better understand the process.[43] The solution pH was adjusted by using 1 M NaOH (Sigma). During ED experiments, a constant direct current of 0.06 A was applied (current density 7.1 mA cm^{-2}), chosen in the ohmic region, and every 30 min aliquots of the solution (5 mL) were collected from both feed and receiving compartments until 120 min. Collected samples were analyzed by ion chromatography (930 Compact IC Flex, 150 mm A Supp 5 column, Metrohm).

In order to evaluate the transport number of each salt (t_{ion}),[37] the following equation was used:[44]

$$t_{ion} = \frac{nFV\frac{dC_{ion}}{dt}}{iA} = \frac{nFJ_{ion}}{i}\ (-) \quad (5)$$

where F is the Faraday constant (96485 C mol^{-1} = 96485 A sec mol^{-1}), n is the valency of the ion, V is the volume of receiving solution (cm^3), C_{ion} is the concentration (mol cm^{-3}) of anion at time t (s), and i is the current density (A cm^{-2}). Considering our experimental conditions (pH 7 and pH 10), we calculated the transport numbers with the assumption of n = 3 for citrate and n = 2 for phosphate, since we assume that monovalent phosphate in the membrane turns into divalent phosphate.[33] All parameters used to calculate transport numbers, including anionic concentrations as from IC, are reported in Tables S1 and S2 in the Supporting Information.

RESULTS AND DISCUSSION

Monomer and Membrane Characterization. The synthesized and purified guanidinium acrylate monomer (Gu-monomer), compound **2**, was analyzed by ^{1}H NMR. The peaks found at δ 7.4 and 6.8 ppm are attributed to the

DOI: 10.1021/acs.est.8b05558
Environ. Sci. Technol. 2019, 53, 2396−2404

guanidinium protons, while peaks at δ 6.4, 6.1, and 5.9 ppm are the characteristic signals of the protons related to the acrylate double bond. FTIR analysis was used to further characterize the structure of compound **2**. In Figure 2, peaks at 3164 and

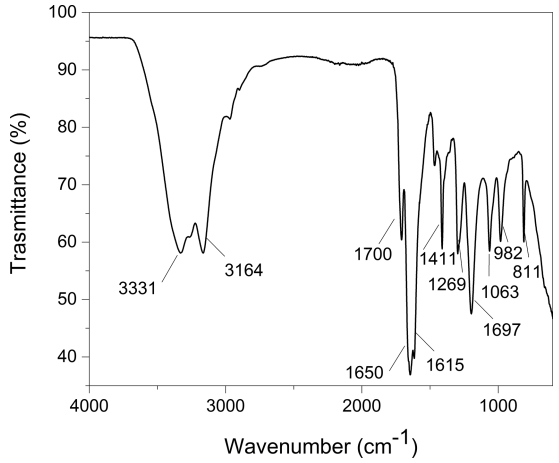

Figure 2. FTIR spectrum of compound **2**. Major peaks are indicated with their wavenumber (cm^{-1}) in the figure and explained in the text.

811 cm^{-1} are associated with the stretching and bending of the N−H bond and the peak at 1650 cm^{-1} is linked to the stretching of the C═N bond, while peaks at 1197 and 1063 cm^{-1} are assigned to the stretching and bending of the N−C bond of the Gu groups.[27,46] The two peaks at 1700 and 1615 cm^{-1} refer to the stretching of the O═C−O and C═C bonds, respectively, indicating the acrylate moiety, and the peak at 1296 cm^{-1} is related to the stretching of the C−O bond of the ester group.[45] Peaks at 3331, 1411, and 982 cm^{-1} are related to the stretching, bending in plane, and bending out of plane of the O−H bond, respectively, originating from the physically adsorbed water of the hydrophilic monomer.[47]

Next, compound **2** was used to fabricate the AEMs, following the procedure described in Materials and Methods. Table 3 reports the composition, the water uptake measurements, and XPS analysis of the Gu-100 and Gu-0 AEMs. The water content is slightly higher for Gu-100 (1.8 wt %) in comparison to Gu-0 (1.5 wt %). Considering the small difference in membrane ion-exchange capacity, we can calculate that ∼37% of water (1 $mmol_{water}/g$, 2.7 $mequiv/g_{Gu\text{-}100}$) for Gu-100 and ∼28% of water (0.8 $mmol_{water}/g$, 2.8 $mequiv/g_{Gu\text{-}0}$) for Gu-0 is associated with the anion-exchanging sites, indicating a slightly higher hydrophilicity for guanidinium groups in comparison to quaternary ammonium. The amounts of nitrogen and carbon at the surface of the membranes were determined by XPS (Table 3) and found to be 6% and 64% for Gu-0 and 12% and 66% for Gu-100 AEM, respectively. Since the ion-exchange site of Gu-0 is a quaternary ammonium group, having one nitrogen atom per site, and that in Gu-100 is a guanidinium group, having three nitrogen atoms per site, the estimated ratio of quaternary ammonium to guanidinium is 5.6:(12.3/3) = 5.6:4.1 = 1.4. From the membrane fabrication, the ratio of quaternary ammonium to guanidinium sites in the (bulk and surface of the) membrane was found to be 2.83:2.71 = 1.04. It is therefore tentatively suggested that the quaternary ammonium groups are more exposed to the membrane surface in comparison to the guanidinium groups. The amounts of found carbon at the membrane surface are comparable for both membranes; the small difference can be associated with some hydrocarbon contamination.[27,48]

Permselectivity and Membrane Electrical Resistance. In Table 4 the permselectivity (PS) results are presented.

Table 4. Permselectivities (% PS) and Observed Membrane Potentials (E_m in mV in Brackets) for Gu-0 and Gu-100 Membranes in the Presence of 0.5/0.05 M of NaCl, NaH_2PO_4, Na_2HPO_4, and Na_2SO_4 Measured Separately

	NaCl	NaH_2PO_4 (pH 5)	Na_2HPO_4 (pH 10)	Na_2SO_4
Gu-0	90.1 [−43]	87.8 [−38]	54.8 [−4.8]	59.5 [−5.7]
Gu-100	87.1 [−40]	72.1 [−22]	−56.4 [3.1]	−55.6 [3.4]

Considering the minor differences observed from the water uptake and anion-exchange capacity values (Table 3), we can assume similar structure densities for Gu-0 and Gu-100. Therefore, we attribute the differences observed in the PS values (Table 4) mainly to the different interactions of the ions with the fixed charge groups of the membranes. An observed positive value of PS (i.e., a negative measured and negative calculated membrane potential) directly indicates that anions are the dominant exchanging, and thus transporting, species in the membrane. This is the situation for Gu-0 in all investigated situations. For the monovalent anions Cl^- and $H_2PO_4^-$ (pH 5) the PS values indicate some co-ion (=cation) uptake. For SO_4^{2-} the observed PS is much lower, indicating a much higher co-ion uptake. It seems that the exchanged SO_4^{2-} acts, in part, as a cation-exchange site. Thus, the quaternary ammonium site is interacting with SO_4^{2-}, resulting in a new, overall negative site that is able to exchange cations (co-ions). To find more evidence for this interpretation, phosphate was also investigated at pH 10, converting the phosphate from the monoanion to the dianion. Indeed, the observed PS is reduced from 88 to 55%. Thus, a phosphate dianion coordinated by the quaternary ammonium group behaves like the sulfate dianion. It is noted that, within this concept, dehydration of the ions is important to enter the membrane and also that the hydration energies of the phosphate dianion and sulfate are similar (−1170 and −1080 kJ/mol, respectively);[49,50] therefore, this does not contribute to the observed differences.

Table 3. Membrane Properties: Type and Number of Exchange Sites, Water Uptake, and Surface Nitrogen and Carbon Composition

	anion-exchange group[a] (mmol/g)			surface composition[b] (atom %)	
AEM	$-N(CH_3)_3^+$	$-Gu^+$	water uptake (wt %; mmol/g)	N	C
Gu-0	2.83	0	1.52 ± 0.05; 0.8	5.6 ± 0.4	64.1 ± 0.1
Gu-100	0	2.71	1.77 ± 0.03; 1.0	12.3 ± 0.1	66.4 ± 0.3

[a]Calculated from membrane fabrication. [b]From XPS analysis.

DOI: 10.1021/acs.est.8b05558
Environ. Sci. Technol. 2019, 53, 2396−2404

For Gu-100 the situation is different. The monovalent ions Cl^- and $H_2PO_4^-$ (pH 5) show PS values similar to those found for Gu-0. The slightly lower PS found for $H_2PO_4^-$ and Gu-100 in comparison to that for Gu-0 might be the result of the expected stronger interaction between $H_2PO_4^-$ and Gu groups (as in Gu-100)[28,33] in comparison to the interaction to the quaternary ammonium (as in Gu-0). For the sulfate and phosphate dianions (at pH 10) a remarkable change in sign of the PS is observed. The negative values directly indicate that the dominant exchanging species is no longer the expected anion. In comparison to monovalent phosphate, divalent phosphate and sulfate interact more strongly with Gu groups. In other words, the observed membrane potential has a positive value, indicating that cations are the dominant exchanging species, while in the calculated Nernst potential we assumed that the anions are dominant, resulting in a calculated negative membrane potential. The situation is more or less similar for sulfate and phosphate dianions. In the Gu-100 membranes, these dianions turn the membranes into cation exchangers: one of the two charges of the counterions binds to the Gu groups, while the second negative charge facilitates the interaction with co-ions, which dominate the overall ion transport. That this happens in the Gu-100 membranes and not (to that extent) in the Gu-0 membranes is attributed to the stronger interaction between both sulfate dianion and phosphate dianion to the Gu groups in comparison to their interaction with quaternary ammonium groups.[33]

In Table 5 the electrical resistances (ERs) of the Gu-0 and Gu-100 membranes are shown as determined by separate experiments using sodium chloride, sodium phosphate (at pH 5 and 10), and sodium sulfate.

Table 5. Observed Electrical Resistances (ERs) for Gu-0 and Gu-100 Membranes in 0.5 M NaCl, NaH_2PO_4 (pH 5), Na_2HPO_4 (pH 10), and Na_2SO_4

	ER (Ω cm^2)[a]			
	NaCl	NaH_2PO_4 (pH 5)	Na_2HPO_4 (pH 10)	Na_2SO_4
Gu-0	1.1	6.3	2.3	1.6
Gu-100	0.9	2.7	1.2	3.0

[a]Error is <5%, on the basis of triplicate measurements.

The lowest ER values are observed for chloride in both Gu-0 and Gu-100, indicating a high mobility of chloride in both membranes having similar properties regarding the number of ion-exchange sites and observed PS. For the phosphate monoanion (pH 5) the situation is different. For Gu-0 the ER value is now higher in comparison to that of chloride. This is in line with the trend in the diffusion coefficients (Table 1): a lower diffusion coefficient results in a lower ion flux through the membrane and hence in a higher ER.[51] For Gu-100 and phosphate (pH 5) the ER is reduced to 2.7 Ω cm^{-2}. This is clearly an effect of the mobile cations (co-ions H^+ and Na^+) in the membrane, as observed/interpreted from the PS data. The phosphate monoanion is expected to be bound more strongly to the guanidinium groups in comparison to the quaternary ammonium groups, thus resulting in an expected lower mobility and hence raising the ER value. The lower ER values can be attributed to these mobile co-ions.

For the sulfate and phosphate dianions (pH 10) the understanding of the observed ER data can be supported by the interpretation of our PS data. In more detail, for Gu-0 we observed a significant amount of co-ion exchange and for Gu-100 the co-ion exchange process was even dominant, as evinced from the recorded positive membrane potential. Thus, for Gu-0 the ER values are determined by a combination of (i) sulfate and phosphate dianions transport, on exchange with the fixed anionic groups of the membrane, and (ii) co-ion (cation) transport. The observed lower ER for HPO_4^{2-} and Gu-100 in comparison to that for Gu-0 might be related to a somewhat larger co-ion uptake for the Gu-100 membranes in comparison to the Gu-0 membranes, as can be deduced from the PS measurements; PS is more negative for Gu-100 in comparison to Gu-0, indicating more co-ion (cation) uptake.

Electrodialysis with Model Dairy Wastewater. Finally, we come to the results of our experiments using the Gu-0 and Gu-100 membranes to separate by electrodialysis a mixed solution containing sodium chloride, sodium phosphate, sodium citrate, sodium lactate, and sodium sulfate, as a model dairy wastewater composition at a common pH 7 and also at pH 10. We are interested in the effect of changing the quaternary ammonium sites (Gu-0) to the guanidinium sites (Gu-100). Before we describe these experiments, a short summary is given of the main properties found for the Gu-0 and Gu-100 membranes. This is done to facilitate the interpretation of the electrodialysis results. Briefly, the amount of sites is similar in both membranes, as is the water uptake. From the PS measurements it was found that exchange of the chloride and phosphate monoanions (pH 5) is hardly

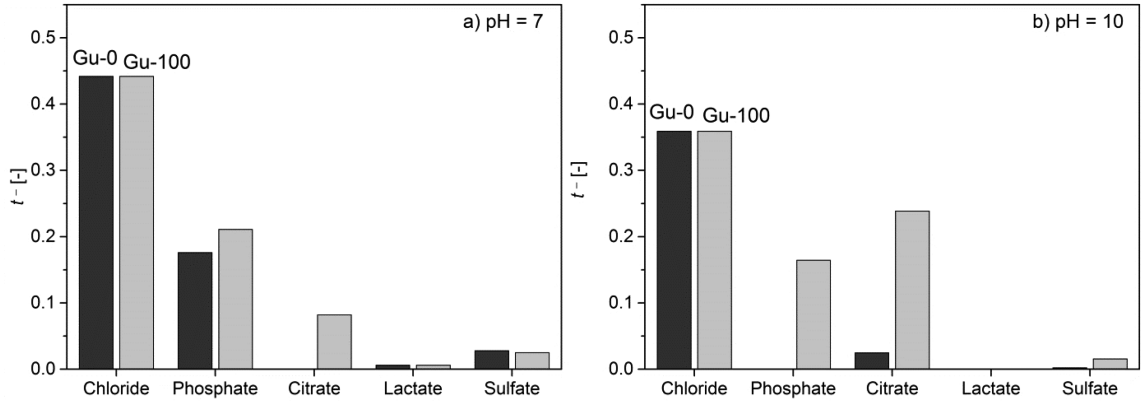

Figure 3. Transport number (t^-) of anions for Gu-0 (black) and Gu-100 (gray) membranes in a model dairy wastewater solution (a) at pH 7 and (b) at pH 10.

DOI: 10.1021/acs.est.8b05558
Environ. Sci. Technol. 2019, 53, 2396−2404

influenced by changing the type of anion-exchange sites in the membrane from quaternary ammonium to guanidinium. The phosphate monoanion (pH 5) is slightly more strongly bound to guanidinium in comparison to quaternary ammonium, as deduced from the observed lower PS (indicating more co-ion uptake). The sulfate and phosphate dianions (pH 10) behave similarly if the membrane is changed from Gu-0 to Gu-100. Both dianions are strongly bound to the guanidinium groups and show a high co-ion uptake. The ER measurements indicate that the mobility of chloride is hardly effected by changing from Gu-0 to Gu-100. Phosphate monoanion (pH 5) is clearly less mobile in comparison to chloride in Gu-0. The ER values for the other situations are all influenced by the co-ion uptake, and the ER value is not directly a measure of the anion mobility in the membranes.

The composition of the model dairy wastewater is given in Table 1 and is shown to (i) be rich in sodium chloride (30 mM), (ii) have equal concentrations of sodium phosphate and sodium citrate (10 mM), and (iii) have low concentrations of sodium lactate and sodium sulfate (both 1 mM).

Both Gu-0 and Gu-100 membranes were operated at an applied constant current of 7.1 mA cm^{-2}, as described in Materials and Methods. Samples from the feed and receiving phase were collected and analyzed by ion chromatography, and the results are represented by their calculated transport numbers (see also eq 5 in Materials and Methods). The results of the ED performed at pH 7 are shown in Figure 3a. The anion transport is dominated by the chloride transport for both Gu-0 and Gu-100. This is as expected because of its high concentration, in comparison to the other present salts, and its low ER value. The transport of lactate and sulfate does play a minor role, due to their very low concentrations in comparison to the other salts present in the model dairy wastewater we applied. Phosphate transport is observed in Gu-0, and the amount transported increases for Gu-100. At pH 7 phosphate is present as a monoanion (62%) and as a dianion (38%) (see Table 2). The present guanidinium groups in Gu-100 are clearly responsible for the increased phosphate transport, as was also deduced from our PS measurements. No citrate transport is found for Gu-0, but it is observed for Gu-100. At pH 7 citrate is present as a dianion (19%) and as a trianion (81%) (see Table 2). Thus, the difference observed between phosphate and citrate transport for Gu-0 can be attributed to the differences in diffusion coefficient (Table 1) and valency; the phosphate monoanion can be exchanged by the quaternary ammonium groups present in Gu-0, while the di- and trianions of citrate cannot. In the presence of guanidinium exchange sites (Gu-100) there is an additional affinity toward the oxyanions (e.g., phosphate), in comparison to quaternary ammonium. This affinity is responsible for the increased uptake and transport of phosphate and citrate at pH 7. To find further support for this interpretation, we have also performed electrodialysis experiments at pH 10. The results are presented in Figure 3b. At this pH, phosphate is present as a dianion (100%) and citrate as a trianion (100%) (see Table 2). It is expected now that the phosphate dianion is also not taken up by the Gu-0 as was citrate before. This is indeed what we have observed: there is a complete absence of any phosphate transport for Gu-0 at pH 10. In the presence of Gu groups (Gu-100) phosphate transport is taking place again. At this pH value also citrate (as trianion) transport is observed for the Gu-100 membranes. It was a surprise to observe some citrate transport under these conditions for the Gu-0 membrane (though only 0.025). We can only speculate why the citrate trianion does transport under these conditions, while the phosphate dianion does not. It is suggested that both citrate and phosphate equilibrate to some extent with the membrane and that the citrate trianion experiences a larger electrophoretic force in comparison to the phosphate dianion.

Finally, for both pH 7 and 10, we can conclude that the uptake of citrate and phosphate is stronger for the Gu-100 membrane in comparison to Gu-0. To obtain more insight into the interaction between the Gu-100 membrane and citrate/phosphate anions, we compare the relative differences in the transport number to the ratio of the diffusivity values (Table 1). We calculate that the diffusivity ratio for phosphate/citrate is 1.2, while the ratio of the transport numbers is 2.6 at pH 7 and 0.69 at pH 10. The difference in the ratio of diffusion coefficients and those of the transport numbers point to a complexation between these anions and the exchange sites of the membrane occurs.

IMPLICATIONS

A new, functionalized anion-exchange membrane containing guanidinium groups as the anion-exchange sites (Gu-100) was made, characterized in detail, and applied in ED experiments. By making use of a functionalized acrylate, we focused on the bulk modification rather than the surface modication[52] or nanomaterial-assisted[53] strategies. This way, high densities of the functional groups in anion- and cation-exhange membranes can be obtained. In the current study, guanidinium groups were chosen as the functional moiety because of their specific interactions with oxyanions: e.g., phosphate. Apart from its relevance in dairy wastewater streams, uncontrolled discharge of P-containing products as present in aqueous streams from agricultural and cosmetic sectors has increased the eutrophication processes: i.e., the rapid growth of aquatic algae in lakes and rivers. Next to the observed increased phosphate transport, the current study also shows an effect of the functionalization of the ion-exchange membrane to the transport of citrate. Citrate is not only an intermediate in the Krebs cycle, it is also used as a chelating agent in water treatment processes and as a descaling agent to remove lime scale.

The synthesis of the functionalized acrylate monomer is based on a two-step modification of a 1-amino-ω-alcohol. This synthesis strategy is not only facile but also modular, as it allows the integration of other functional moieties. As such, the presented approach has the potential to prepare ion-exchange membranes that address other ions that are environmentally relevant. As a final remark, it is noted that functionalized anion- and cation-exchange membranes are not only relevant for ED processes but also of importance in other fields, including those of fuel cells and capacitive deionization. This further illustrates the (environmental) scope of the ability to control the selective transport of ions.

ASSOCIATED CONTENT

Supporting Information

The Supporting Information is available free of charge on the ACS Publications website at DOI: 10.1021/acs.est.8b05558.

Illustration of the permselectivity setup, parameters used to calculate the anionic transport numbers, and ion chromatography data (PDF)

DOI: 10.1021/acs.est.8b05558
Environ. Sci. Technol. 2019, 53, 2396−2404

AUTHOR INFORMATION

Corresponding Authors

*E-mail for L.P.: l.paltrinieri@tudelft.nl.
*E-mail for L.C.P.M.d.S.: louis.desmet@wur.nl.

ORCID

Laura Paltrinieri: 0000-0003-4544-7984
Ernst J.R. Sudhölter: 0000-0003-3296-953X
Louis C. P. M. de Smet: 0000-0001-7252-4047

Present Address

#W.v.B.: Water Future B.V., Sint Josephstraat 76, 5104 EG Dongen, The Netherlands.

Notes

The authors declare no competing financial interest.

ACKNOWLEDGMENTS

The authors thank Wetsus—European centre of excellence for sustainable water technology (Leeuwarden, The Netherlands) financial support. This study was partially supported by the European Research Council (ERC Consolidator Grant 682444, E-motion, PI L.C.P.M.d.S.). Dr. Henk Miedema, Dr. Jan Post (Wetsus), and the other members of the Desalination theme of Wetsus are thanked for their support and fruitful discussions, and Zexin Qian is thanked for the IC analysis and Lars van der Mee for the LC-MS analysis.

REFERENCES

(1) Hudson, J. J.; Taylor, W. D.; Schindler, D. W. Phosphate Concentrations in Lakes. *Nature* **2000**, *406*, 54−56.
(2) Service, R. F. Desalination Freshens Up. *Science* **2006**, *313* (5790), 1088−1090.
(3) Strathmann, H. Electrodialysis, a Mature Technology with a Multitude of New Applications. *Desalination* **2010**, *264*, 268−288.
(4) Dlugolecki, P.; van der Wal, A. Energy Recovery in Membrane Capacitive Deionization. *Environ. Sci. Technol.* **2013**, *47* (9), 4904−4910.
(5) AlMarzooqi, F. A.; Al Ghaferi, A. A.; Saadat, I.; Hilal, N. Application of Capacitive Deionisation in Water Desalination: A Review. *Desalination* **2014**, *342*, 3−15.
(6) Dlugolecki, P.; Nijmeijer, K.; Metz, S.; Wessling, M. Current Status of Ion Exchange Membranes for Power Generation from Salinity Gradients. *J. Membr. Sci.* **2008**, *319*, 214−222.
(7) Galama, A. H.; Vermaas, D. A.; Veerman, J.; Saakes, M.; Rijnaarts, H. H. M.; Post, J. W.; Nijmeijer, K. Membrane Resistance: The Effect of Salinity Gradients over a Cation Exchange Membrane. *J. Membr. Sci.* **2014**, *467*, 279−291.
(8) Chen, G. Electrochemical Technologies in Wastewater Treatment. *Sep. Purif. Technol.* **2004**, *38*, 11−41.
(9) Liu, R.; Wang, Y.; Wu, G.; Luo, J.; Wang, S. Development of a Selective Electrodialysis for Nutrient Recovery and Desalination during Secondary Effluent Treatment. *Chem. Eng. J.* **2017**, *322*, 224−233.
(10) Zhang, Y.; Van der Bruggen, B.; Pinoy, L.; Meesschaert, B. Separation of Nutrient Ions and Organic Compounds from Salts in RO Concentrates by Standard and Monovalent Selective Ion-Exchange Membranes Used in Electrodialysis. *J. Membr. Sci.* **2009**, *332*, 104−112.
(11) Strathmann, H. Ion-Exchange Membrane Processes in Water Treatment. *Sustain. Sci. Eng. Elsevier* **2010**, *2*, 141−199.
(12) Chapotot, A.; Lopez, V.; Lindheimer, A.; Aouad, N.; Gavach, C. Electrodialysis of Acid Solutions with Metallic Divalent Salts: Cation-Exchange Membranes with Improved Permeability to Protons. *Desalination* **1995**, *101*, 141−153.
(13) Bazinet, L. Electrodialytic Phenomena and Their Applications in the Dairy Industry: A Review. *Crit. Rev. Food Sci. Nutr.* **2005**, *45* (4), 307−326.
(14) Boniardi, N.; Rota, R.; Nano, G.; Mazza, B. Analysis of the Sodium Lactate Concentration Process by Electrodialysis. *Sep. Technol.* **1996**, *6* (1), 43−54.
(15) Fidaleo, M.; Moresi, M. Concentration of Trisodium Citrate by Electrodialysis. *J. Membr. Sci.* **2013**, *447*, 376−386.
(16) Andrés, L. J.; Riera, F. A.; Alvarez, R. Skimmed Milk Demineralization by Electrodialysis: Conventional versus Selective Membranes. *J. Food Eng.* **1995**, *26* (1), 57−66.
(17) van der Horst, H. C.; Timmer, J. M. K.; Robbertsen, T.; Leenders, J. Use of Nanofiltration for Concentration and Demineralization in the Dairy Industry: Model for Mass Transport. *J. Membr. Sci.* **1995**, *104*, 205−218.
(18) Zhang, Y.; Desmidt, E.; Van Looveren, A.; Pinoy, L.; Meesschaert, B.; Van Der Bruggen, B. Phosphate Separation and Recovery from Wastewater by Novel Electrodialysis. *Environ. Sci. Technol.* **2013**, *47* (11), 5888−5895.
(19) Luo, T.; Abdu, S.; Wessling, M. Selectivity of Ion Exchange Membranes: A Review. *J. Membr. Sci.* **2018**, *555*, 429−454.
(20) White, N.; Misovich, M.; Yaroshchuk, A.; Bruening, M. L. Coating of Nafion Membranes with Polyelectrolyte Multilayers to Achieve High Monovalent/divalent Cation Electrodialysis Selectivities. *ACS Appl. Mater. Interfaces* **2015**, *7* (12), 6620−6628.
(21) Mulyati, S.; Takagi, R.; Fujii, A.; Ohmukai, Y.; Matsuyama, H. Simultaneous Improvement of the Monovalent Anion Selectivity and Antifouling Properties of an Anion Exchange Membrane in an Electrodialysis Process, Using Polyelectrolyte Multilayer Deposition. *J. Membr. Sci.* **2013**, *431*, 113−120.
(22) Rijnaarts, T.; Shenkute, N. T.; Wood, J. A.; de Vos, W. M.; Nijmeijer, K. Divalent Cation Removal by Donnan Dialysis for Improved Reverse Electrodialysis. *ACS Sustainable Chem. Eng.* **2018**, *6* (5), 7035−7041.
(23) Kim, D. H.; Park, H. S.; Seo, S. J.; Park, J. S.; Moon, S. H.; Choi, Y. W.; Jiong, Y. S.; Kim, D. H.; Kang, M. S. Facile Surface Modification of Anion-Exchange Membranes for Improvement of Diffusion Dialysis Performance. *J. Colloid Interface Sci.* **2014**, *416*, 19−24.
(24) Lee, W.; Saito, K.; Furusaki, S.; Sugo, T.; Makuuchi, K. Design of Urea-Permeable Anion-Exchange Membrane by Radiation-Induced Graft Polymerization. *J. Membr. Sci.* **1993**, *81*, 295−306.
(25) Hosseini, S. M.; Nemati, M.; Jeddi, F.; Salehi, E.; Khodabakhshi, R.; Madaeni, S. S. Fabrication of Mixed Matrix Heterogeneous Cation Exchange Membrane Modified by Titanium Dioxide Nanoparticles: Mono/bivalent Ionic Transport Property in Desalination. *Desalination* **2015**, *359*, 167−175.
(26) Pantos, A.; Tsogas, I.; Paleos, C. M. Guanidinium Group: A Versatile Moiety Inducing Transport and Multicompartmentalization in Complementary Membranes. *Biochim. Biophys. Acta, Biomembr.* **2008**, *1778*, 811−823.
(27) Paltrinieri, L.; Wang, M.; Sachdeva, S.; Besseling, N. A. M.; Sudhölter, E. J. R.; de Smet, L. C. P. M. Fe3O4 Nanoparticles Coated with a Guanidinium-Functionalized Polyelectrolyte Extend the pH Range for Phosphate Binding. *J. Mater. Chem. A* **2017**, *5*, 18476−18485.
(28) Cao, Z.; Gordiichuk, P. I.; Loos, K.; Sudhölter, E. J. R.; de Smet, L. C. P. M. Effect of Guanidinium Functionalization on the Structural Properties and Anion Affinity of Polyelectrolyte Multilayers. *Soft Matter* **2016**, *12*, 1496−1505.
(29) Liu, L.; Li, Q.; Dai, J.; Wang, H.; Jin, B.; Bai, R. A Facile Strategy for the Synthesis of Guanidinium-Functionalized Polymer as Alkaline Anion Exchange Membrane with Improved Alkaline Stability. *J. Membr. Sci.* **2014**, *453*, 52−60.
(30) Park, J.; Yi, J.; Tachikawa, T.; Majima, T.; Choi, W. Guanidinium-Enhanced Production of Hydrogen on Nafion-Coated Dye/TiO 2 under Visible Light. *J. Phys. Chem. Lett.* **2010**, *1* (9), 1351−1355.
(31) Zhang, Q.; Li, S.; Zhang, S. A Novel Guanidinium Grafted Poly(aryl Ether Sulfone) for High-Performance Hydroxide Exchange Membranes. *Chem. Commun. (Cambridge, U. K.)* **2010**, *46* (40), 7495−7497.

DOI: 10.1021/acs.est.8b05558
Environ. Sci. Technol. 2019, 53, 2396−2404

(32) Sajjad, S. D.; Hong, Y.; Liu, F. Synthesis of Guanidinium-Based Anion Exchange Membranes and Their Stability Assessment. *Polym. Adv. Technol.* **2014**, *25*, 108−116.
(33) Paltrinieri, L.; Poltorak, L.; Chu, L.; Puts, T.; van Baak, W.; Sudhölter, E. J. R.; de Smet, L. C. P. M. Hybrid Polyelectrolyte-Anion Exchange Membrane for Phosphate Removal. *React. Funct. Polym.* **2018**, *133*, 126−135.
(34) Funhoff, A. M.; van Nostrum, C. F.; Lok, M. C.; Fretz, M. M.; Crommelin, D. J.a; Hennink, W. E. Poly(3-Guanidinopropyl Methacrylate): A Novel Cationic Polymer for Gene Delivery. *Bioconjugate Chem.* **2004**, *15* (6), 1212−1220.
(35) Sata, T. *Ion Exchange Membranes Preparation, Characterization, Modification and Application*; RSC: 2004.
(36) Sata, T. Studies on Ion Exchange Membranes with Permselectivity for Specific Ions in Electrodialysis. *J. Membr. Sci.* **1994**, *93*, 117−135.
(37) Sata, T. Studies on Anion Exchange Membranes Having Permselectivity for Specific Anions in Electrodialysis - Effect of Hydrophilicity of Anion Exchange Membranes on Permselectivity of Anions. *J. Membr. Sci.* **2000**, *167*, 1−31.
(38) Geise, G. M.; Cassady, H. J.; Paul, D. R.; Logan, B. E.; Hickner, M. A. Specific Ion Effects on Membrane Potential and the Permselectivity of Ion Exchange Membranes. *Phys. Chem. Chem. Phys.* **2014**, *16* (39), 21673−21681.
(39) Cassady, H. J.; Cimino, E. C.; Kumar, M.; Hickner, M. A. Specific Ion Effects on the Permselectivity of Sulfonated Poly(ether Sulfone) Cation Exchange Membranes. *J. Membr. Sci.* **2016**, *508*, 146−152.
(40) Dlugolecki, P.; Ogonowski, P.; Metz, S. J.; Saakes, M.; Nijmeijer, K.; Wessling, M. On the Resistances of Membrane, Diffusion Boundary Layer and Double Layer in Ion Exchange Membrane Transport. *J. Membr. Sci.* **2010**, *349*, 369−379.
(41) Geise, G. M.; Hickner, M. A.; Logan, B. E. Ionic Resistance and Permselectivity Tradeoffs in Anion Exchange Membranes. *ACS Appl. Mater. Interfaces* **2013**, *5*, 10294−10301.
(42) Galama, A. H.; Hoog, N. A.; Yntema, D. R. Method for Determining Ion Exchange Membrane Resistance for Electrodialysis Systems. *Desalination* **2016**, *380*, 1−11.
(43) Sarapulova, V.; Nevakshenova, E.; Pismenskaya, N.; Dammak, L.; Nikonenko, V. Unusual Concentration Dependence of Ion-Exchange Membrane Conductivity in Ampholyte-Containing Solutions: Effect of Ampholyte Nature. *J. Membr. Sci.* **2015**, *479*, 28−38.
(44) Güler, E.; van Baak, W.; Saakes, M.; Nijmeijer, K. Monovalent-Ion-Selective Membranes for Reverse Electrodialysis. *J. Membr. Sci.* **2014**, *455*, 254−270.
(45) Lide, D. R. *CRC Handbook of Chemistry and Physics*, 84th ed.; CRC Press: 2003; Vol. 53, p 2616.
(46) Tristán, F.; Palestino, G.; Menchaca, J.-L.; Pérez, E.; Atmani, H.; Cuisinier, F.; Ladam, G. Tunable Protein-Resistance of Polycation-Terminated Polyelectrolyte Multilayers. *Biomacromolecules* **2009**, *10* (8), 2275−2283.
(47) Wong, J. E.; Gaharwar, A. K.; Müller-Schulte, D.; Bahadur, D.; Richtering, W. Magnetic Nanoparticle-Polyelectrolyte Interaction: A Layered Approach for Biomedical Applications. *J. Nanosci. Nanotechnol.* **2008**, *8* (8), 4033−4040.
(48) Stevens, J. S.; De Luca, A. C.; Pelendritis, M.; Terenghi, G.; Downes, S.; Schroeder, S. L. M. Quantitative Analysis of Complex Amino Acids and RGD Peptides by X-Ray Photoelectron Spectroscopy (XPS). *Surf. Interface Anal.* **2013**, *45*, 1238−1246.
(49) Eiberweiser, A.; Nazet, A.; Hefter, G.; Buchner, R. Ion Hydration and Association in Aqueous Potassium Phosphate Solutions. *J. Phys. Chem. B* **2015**, *119* (16), 5270−5281.
(50) Smith, D. W. Ionic Hydration Enthalpies. *J. Chem. Educ.* **1977**, *54* (9), 540−542.
(51) Kamcev, J.; Paul, D. R.; Manning, G. S.; Freeman, B. D. Ion Diffusion Coefficients in Ion Exchange Membranes: Significance of Counterion Condensation. *Macromolecules* **2018**, *51* (15), 5519−5529.
(52) Khoiruddin; Ariono, D.; Subagjo; Wenten, I. G. Surface Modification of Ion-Exchange Membranes: Methods, Characteristics, and Performance. *J. Appl. Polym. Sci.* **2017**, *134*, 45540.
(53) Alabi, A.; AlHajaj, A.; Cseri, L.; Szekely, G.; Budd, P.; Zou, L. Review of Nanomaterials-Assisted Ion Exchange Membranes for Electromembrane Desalination. *npj Clean Water* **2018**, *1*, 10.

DOI: 10.1021/acs.est.8b05558
Environ. Sci. Technol. 2019, 53, 2396−2404